



## Neutron diffraction studies of $Gd_2Zr_2O_7$ pyrochlore

Brendan J. Kennedy<sup>a,\*</sup>, Qingdi Zhou<sup>a</sup>, Maxim Avdeev<sup>b</sup>

<sup>a</sup> School of Chemistry, The University of Sydney, Sydney, NSW 2006, Australia

<sup>b</sup> Bragg Institute, Australian Nuclear Science and Technology Organisation, Private Mail Bag 1, Menai, NSW 2234, Australia

### ARTICLE INFO

#### Article history:

Received 11 January 2011

Received in revised form

27 March 2011

Accepted 4 April 2011

Available online 12 May 2011

#### Keywords:

Pyrochlore

Anion disorder

Neutron diffraction

<sup>160</sup>Gd

Radiation damage

### ABSTRACT

The structure of  $Gd_2Zr_2O_7$  pyrochlore over the temperature range 4–300 K has been refined from powder neutron diffraction data. The sample was enriched in <sup>160</sup>Gd to avoid the high neutron absorption of naturally occurring Gd. The diffraction pattern showed well resolved superlattice reflections indicative of the pyrochlore structure and no evidence is found for anion-disorder from the structural refinements.

© 2011 Elsevier Inc. All rights reserved.

### 1. Introduction

Questions over the sustainability of the carbon fuel cycle are driving research into alternate methods to generate electricity. Pyrochlore oxides are attracting considerable attention for their potential use in two possible replacement technologies, namely as electrolytes in solid oxide fuel cells [1] and components in the nuclear fuel cycle, both as host matrices for actinide wastes [2] or in inert matrix fuels [3]. One particular composition,  $Gd_2Zr_2O_7$ , is being actively explored for both technologies due to its high ionic conductivity; La doped- $Gd_2Zr_2O_7$  has conductivity  $\sigma_{dc}$  values similar to those of Y doped  $ZrO_2$  [1], and displays excellent resistance to radiation induced amorphization [4]. Although the applications are vastly different the suitability of  $Gd_2Zr_2O_7$  in both fields can be rationalised from its structure. The general stoichiometry of pyrochlores is often written as  $A_2B_2O_6O'$  (in space group  $Fd\bar{3}m$  No. 227) and can be described as a superstructure of the  $AO_2$  fluorite structure ( $Fm\bar{3}m$  No. 225) where the anion vacancies and two cations are ordered, as illustrated in Fig. 1 [5]. There are four equivalent ways to describe a pyrochlore structure in  $Fd\bar{3}m$ . Here we have placed the larger A-cations on the 16d at 1/2 1/2 1/2 and the smaller B-cations on 16c at 0 0 0. There are two types of anions in the ideal pyrochlore structure and these are typically distinguished by their Wyckoff labels, 48f and 8b. The anions at the 48f site are at a distance of about 2 Å from the smaller B-type cations, and these from a network of corner sharing  $BO_6$  octahedra. The A-type cations fill the resulting

interstices and are  $\sim 2.4$ – $2.6$  Å, from the 48f sites. The anions on the 8b site form a  $Cu_2O$  type chain with the B-type cations with the B–O distance being around 1.9–2.1 Å. The corresponding 8a site is vacant.

The stability of the pyrochlore structure is generally related to the ratio of the ionic radii of the A- and B-type cations, and is normally observed for  $r_A/r_B=1.46$ – $1.78$ . Typically smaller values of  $r_A/r_B$  favour the formation of the disordered fluorite-type structure [5]. The  $r_A/r_B$  value of  $Gd_2Zr_2O_7$  is near to the limit of pyrochlore stability, 1.46. A second structural consideration is that in the pyrochlore structure all the atoms, including the oxygen at 48f, occupy special positions; such that the single positional coordinate  $x_{48f}$  together with the cubic lattice parameter fully describe the structure. When  $x_{48f}$  equals 0.375 the structure would be a “perfect” defect-fluorite. The precise values of  $x_{48f}$  in  $Gd_2Zr_2O_7$  is unknown although Moriga et al. [6] reported a value of 0.3411(9) using single crystal X-ray methods. Lian et al. [7] described  $Gd_2Zr_2O_7$  as adopting a disordered defect fluorite structure with  $x_{48f}=0.345$ , whilst Mandal et al. [8] reported  $x_{48f}=0.332(1)$ . Lee et al. [9] suggest that the precise location of the 48f anion is dependent on the extent of anion disorder, shifting from near 0.347(1) in ordered samples to 0.359(1) in extensively disordered samples.

The ordered  $Gd_2Zr_2O_7$  pyrochlore structure has a strong propensity to transform to the disordered fluorite structure and it is reported to undergo a first order pyrochlore to fluorite transition at about 1550 °C [10]. This transition is unusual in that it involves the simultaneous disordering of the cations and anions. There is some evidence that the cation and anion sublattices can be disordered independently by thermal treatment and chemical substitution [11]. Computational studies show

\* Corresponding author. Fax: +61 2 9351 3329.

E-mail address: [b.kennedy@chem.usyd.edu.au](mailto:b.kennedy@chem.usyd.edu.au) (B.J. Kennedy).

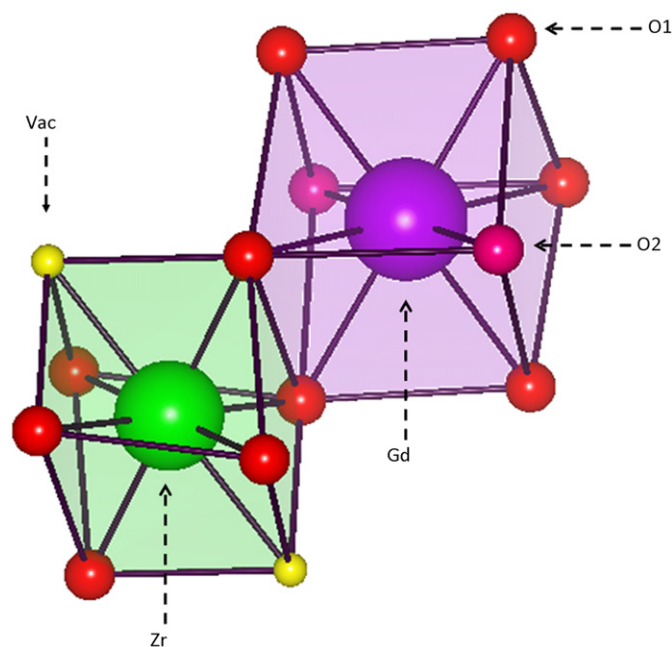


**Fig. 1.** Representation of the  $\text{GdO}_6$  and  $\text{ZrO}_6$  polyhedra in the  $\text{Gd}_2\text{Zr}_2\text{O}_7$  pyrochlore structure. The larger spheres represent the cations. The 48f and 8b anion sites are occupied by the oxygen anions whilst the 8a sites are vacant in the ideal pyrochlore.

the increase in the ionic conductivity in pyrochlore is most likely a consequence of increased vacancies at the 48f site as a result of cation and anion disorder [12]. Furthermore anion Frenkel defects are easily formed [13] in  $\text{Gd}_2\text{Zr}_2\text{O}_7$  hence accounting for the ionic conductivity in this material.

The suitability of  $\text{Gd}_2\text{Zr}_2\text{O}_7$  as a nuclear material centres around its resistance to radiation-induced amorphization. There is considerable debate as to how this occurs, but it appears that ease of the relaxation of the defects formed upon radiation is important and it can be speculated that this will reflect the ease of transformation to the fluorite structure. Lian et al. [7] suggested that the radiation resistance of  $\text{Ln}_2\text{Zr}_2\text{O}_7$  oxides is dependent on the extent of deviation from an ideal fluorite structure ( $\chi_{48f}=0.375$ ). As the structure approaches the ideal, ordered pyrochlore structure, radiation-induced amorphization is more easily attained [14]. The reported range of  $\chi_{48f}$  values 0.332–0.359 in  $\text{Gd}_2\text{Zr}_2\text{O}_7$  is expected to correspond to significant differences in stability. The transformation to the fluorite involves disordering of both the cations and anions; however, there is limited direct evidence for cation antisite (AB-site mixing) disorder in pyrochlores.

Why is so-little known about the position and ordering of the anions in  $\text{Gd}_2\text{Zr}_2\text{O}_7$ ? X-ray diffraction data, which is most commonly used to refine structures, involves scattering from the electron cloud. The high atomic numbers of Gd and Zr means both cations are considerably stronger scatterers of X-rays than the oxygen atoms. Neutron diffraction should be superior to X-ray diffraction since in neutron diffraction measurements the scattering of the oxygen is comparable to that of Gd and Zr, however naturally occurring Gd has an extremely high neutron absorption cross section and this generally precludes the use of such methods. There have been a number of attempts to overcome this problem. Since it is generally assumed that the lanthanide cations in pyrochlores can be considered as purely ionic it is a reasonable postulate that the Gd could be modelled through the use of a suitable mixture of a larger and smaller lanthanide cation. A small number of studies of solid solutions  $\text{Ln}_{2-x}\text{Ln}'_x\text{Zr}_2\text{O}_7$ , where Ln and Ln' are lanthanide cations being larger and smaller than Gd, respectively, have demonstrated

that this approach induces the pyrochlore–fluorite transition [15,16]. Of relevance to the current work we have recently characterised the series  $\text{Nd}_{2-x}\text{Ho}_x\text{Zr}_2\text{O}_7$  using neutron diffraction methods and revealed the presence of extensive anion disorder in the pyrochlore phase [17].

In the present study we have exploited the observation that not all isotopes of Gd strongly absorb neutrons and through the use of suitably enriched oxides it is possible to use neutron diffraction methods. The absorption coefficient for  $^{160}\text{Gd}$  is listed as 0.77 barn which is a factor of  $10^5$  smaller than that of  $^{157}\text{Gd}$ , the most strongly absorbing isotope of Gd.  $^{160}\text{Gd}$  is also somewhat more abundant than  $^{157}\text{Gd}$  (21.9% vs 15.7%). In the present case we have used high resolution neutron powder diffraction (NPD) to establish the structure of  $\text{Gd}_2\text{Zr}_2\text{O}_7$  using a sample enriched in  $^{160}\text{Gd}$ .

## 2. Experimental

$^{160}\text{Gd}_2\text{O}_3$  (~0.7 g) (Isoflex 99.8% isotope purity) was preheated at 1000 °C for 3 h and  $\text{ZrO}_2$  (99.99%) were preheated at 1000 °C for 12 h, to remove any  $\text{H}_2\text{O}$ , before use. The two oxides were mixed by hand and heated at 1000 °C for 20 h. The resulting powder was then re-ground and pressed into a pellet that was then heated at 1450 °C for 15 days with an intermediate re-mixing. The sample was sealed in a 6 mm diameter vanadium can and neutron powder diffraction data were obtained using the high resolution powder diffractometer Echidna [18] at ANSTO's OPAL facility at Lucas Heights. The wavelength of the incident neutrons, obtained using a Ge 335 monochromator, was 1.622 Å as determined using data collected for a certified NIST SRM676  $\text{Al}_2\text{O}_3$  standard. This instrument has a maximum resolution of  $\Delta d/d \sim 1 \times 10^{-3}$ , with data collection taking around 8 h. Patterns to lower statistics were obtained at temperatures between 4 and 300 K in order to establish the temperature dependence of the structure.

The structure was refined using the Rietveld method implemented in the programme GSAS [19,20]. The neutron peak shape was modelled using a pseudo-Voigt function and the background was estimated using an eight-term shifted Chebyshev function. Anisotropic displacement parameters were refined for the oxygen anions. The neutron scattering length of  $^{160}\text{Gd}$  used in the Rietveld analysis was 8.922 fm, this value being obtained from analysis of neutron diffraction data collected for the  $^{160}\text{Gd}_2\text{O}_3$  starting material [17].

## 3. Results and discussion

The neutron powder diffraction (NPD) pattern demonstrates that the present sample of  $^{160}\text{Gd}_2\text{Zr}_2\text{O}_7$  adopts the cubic pyrochlore structure in space group  $Fd\bar{3}m$ . Although there have been a small number of neutron diffraction studies reported for  $^{160}\text{Gd}$  enriched samples [21–25], the methodology is still sufficiently novel that some comment on the choice of scattering length is appropriate. The strategy we employed was to record a neutron data-set from the same batch of  $^{160}\text{Gd}_2\text{O}_3$  employed in the synthesis of  $\text{Gd}_2\text{Zr}_2\text{O}_7$ . The scattering length of the Gd was allowed to freely vary in the refinement of the structure of  $\text{Gd}_2\text{O}_3$  from this data, and this gave a value of 8.922 fm [17]. The tabulation by Sears [26] lists a value of 9.15 fm, the difference (about 2.5%) between the two values probably arises from a combination of experimental uncertainties and the precise isotopic composition of the samples studied.

The structure of  $^{160}\text{Gd}_2\text{Zr}_2\text{O}_7$  at both 4 and 300 K was refined from NPD and the results are presented in Table 1. Fig. 2 illustrates the quality of the fit to the 4 K data-set. The possibility

**Table 1**

Crystallographic parameters for  $Gd_2Zr_2O_7$ . Where two values are given the first value refers to the structure at 4 K and the second value that at 295 K. The number in parentheses beside each entry indicates the estimated standard deviation refer to the last digit shown. The anisotropic displacement parameters for O(1) are listed.

Atom	Site	x	y	z	$U_{eq}$ (100 Å <sup>2</sup> )
Gd	16d	1/2	1/2	1/2	0.31(7) 1.6(2)
Zr	16c	0	0	0	1.11(11) 2.4(2)
O1	48f	0.3456(3) 0.3476(7)	1/8	1/8	2.08* 3.84*
O2	8b	3/8	3/8	3/8	0.5(3) 1.9(6)

$U^{11}=3.8(3)$   $U^{12}=1.2(1)$   $U^{23}=0.6(2)$  @ 4 K  $U^{11}=4.4(5)$   $U^{12}=3.6(3)$   $U^{23}=0.4(4)$  @ RT.

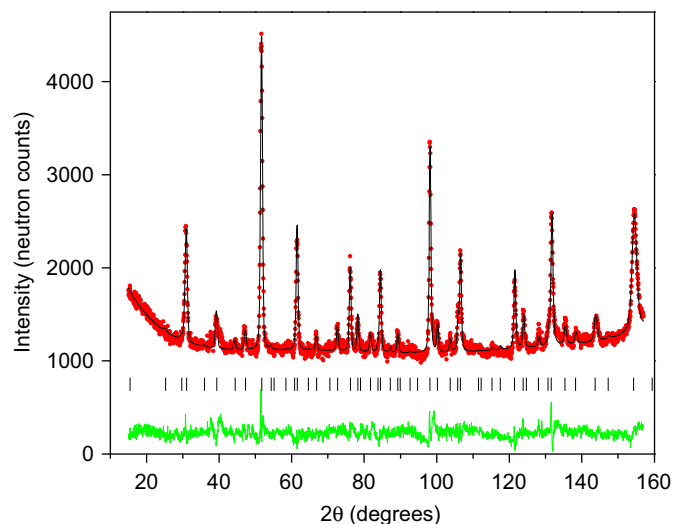


**Fig. 2.** Neutron diffraction pattern recorded at 4 K from  $Gd_2Zr_2O_7$  enriched in  $^{160}Gd$ . The circles represent the observed data and the continuous line is the fit obtained by the Rietveld method using the cubic structure in  $Fd\bar{3}m$ . The vertical marks show peak positions expected in this structure and the line beneath the pattern is the difference between the observed and calculated patterns. The higher than typical background is likely due to the small size of the sample and incoherent scattering by traces of other Gd isotopes present in the sample.

that some of the oxygen disordered from the 48f to the nominally vacant 8a site was also investigated, however the refinements indicated this did not occur. The absence of such disorder in this sample is believed to be a consequence of the temperature used to anneal the sample.

The structure of  $Gd_2Zr_2O_7$  has been refined from X-ray powder diffraction data by a number of workers, resulting in a range of values for  $x_{48f}$ ,  $\sim 0.332$ – $0.359$ . Although limited the results described by Lee et al. [9] suggest that the precise location of the 48f anion is dependent on the extent of anion disorder, shifting from near 0.347(1) in ordered samples to 0.359(1) in extensively disordered samples [9]. The present results demonstrate that in a sample lacking appreciable anion disorder the value of  $x_{48f}$  is 0.3456(3). This value is statistically different to that obtained by Moriga et al. [6] in their single crystal XRD study of  $Gd_2Zr_2O_7$ , 0.3411(9), and represents a reduction in the trigonal distortion of the  $ZrO_6$  moiety. It should be noted that Moriga [6] reported solutions for two crystals, the first of which was annealed at 1550 °C and was free of diffuse features in precession photographs. Their second crystal was annealed at 1600 °C and displayed obvious diffuse feature in the precession photographs

indicative of disorder. There are no obvious diffuse features in the observed neutron profiles of our sample which was annealed at 1450 °C and so the comparison with the results for the sample labelled S by Moriga [6] appear reasonable. It has been recently demonstrated that the degree of disorder in  $Gd_2Zr_2O_7$  is sensitive to the thermal history of the material. When prepared at low temperatures  $Gd_2Zr_2O_7$  adopts a defect fluorite structure and this transforms to disordered pyrochlore at temperatures higher than 1200 °C in static air environment [27]. It seems a reasonable postulate that  $x \sim 0.346$  in well ordered  $Gd_2Zr_2O_7$  (Table 2).

The Gd cations in  $Gd_2Zr_2O_7$  are in a compressed scalenohedral environment. The Gd–O(1) distance, 2.458(4) Å, is significantly longer than the two Gd–O(2) bonds, along the  $-3$  axis, 2.28200(7) Å reflecting a relatively weak interaction between the Gd and the  $Zr_2O_6$  network. The Zr cations are surrounded by six O(1) atoms in a trigonal antiprism geometry with six equal Zr–O(1) distances of 2.130(3) Å. There was no evidence, from the neutron diffraction data, or from an XRD pattern recorded for a sample containing natural Gd, and prepared under identical conditions, for disorder of the Gd cations, analogous to that found in  $La_2Zr_2O_7$  [28] or in Bi containing pyrochlores [29]. The bond valence sums for Zr (3.70) and Gd (3.29) are both slightly different to their ideal values reflecting the proximity of the material to the pyrochlore-fluorite phase boundary. The Zr–O(1)–Zr angle is 122.07(32)°. This angle is smaller than that found for  $Gd_2Sn_2O_7$  128.8°, [30] reflecting the size difference between  $Zr^{4+}$  (0.72 Å) and  $Sn^{4+}$  (0.69 Å) [31] and is appreciably smaller than the 133.17° found for the metallic oxide  $Bi_2Ru_2O_7$  [32].

The cubic lattice parameter for  $Gd_2Zr_2O_7$  is essentially independent of temperature below 50 K and increases sharply above this (Fig. 3). The oxygen (1) anion positional parameter  $x_{48f}$  shows

**Table 2**

Selected bond distances and angles for  $Gd_2Zr_2O_7$  at 4 and 295 K.

Temp (K)	4	295
$a$ (Å)	10.5249(2)	10.54010(4)
$R_p$ (%)	4.00	9.57
$R_{wp}$ (%)	3.09	10.24
$\chi^2$	2.07	1.48
Gd–O(1) (Å)	2.471(2)	2.458(4)
Gd–O(2) (Å)	2.27871(3)	2.28200(7)
Zr–O1 (Å)	2.115(2)	2.130(3)
Gd–Gd (Å)	3.72111(7)	3.72649(11)
Zr–O–Zr (deg.)	123.21(17)	122.07(32)

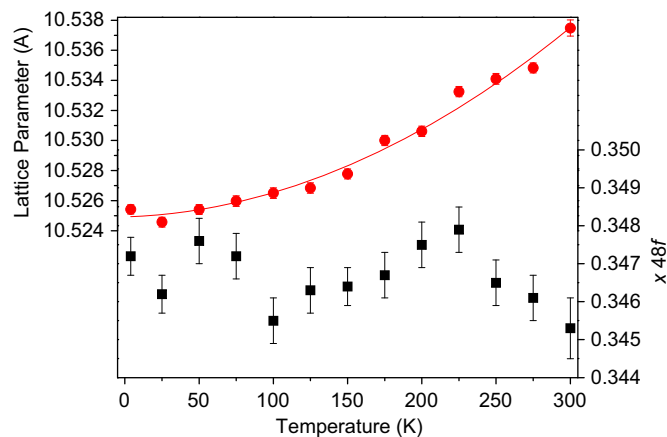


**Fig. 3.** Temperature dependence of the cubic lattice parameter (circles) and  $x_{48f}$  (squares) for  $Gd_2Zr_2O_7$  obtained from Rietveld refinement of powder neutron diffraction data. Where not apparent the esds are smaller than the symbols. The solid curve is a guide to the eye.

a very small increase upon cooling, although the spread of values is comparable to the statistical errors. This small increase in  $x$  effectively compensates for the contraction in the unit cell such that the Zr–O(1) and Gd–O(1) distances remain effectively constant over this temperature range. Only the Gd–O(2) bond distance exhibits a systematic change, this being given by the expression  $d=(3^{1/2}a/8)$ . Despite the rapid increase in cell size above 100 K the all other interatomic contacts in  $Gd_2Zr_2O_7$  remain independent of temperature. All the atomic displacement parameters systematically increased as the temperature was raised from 4 K, but no anomalies were apparent suggesting that although energetically the sample is close to the pyrochlore–fluorite phase boundary the kinetics of such a transition are likely to be very slow under ambient conditions.

Although the radius ratio  $r_A/r_B$  is generally regarded as the dominate influence for the formation of the pyrochlore structure and its transformation to a disordered fluorite state, it is interesting to note that the presence of strong covalent bonding apparently inhibits the order–disorder structural transition as evident from studies of solid solutions such as  $Y_2(Sn_xTi_{2-x})O_7$  and  $Gd_2(Sn_xTi_{2-x})O_7$  over the same range of  $r_A/r_B$  values in the  $Ln_2(Zr,Ti)_2$  solid solution [33]. Through the use of  $^{160}Gd$  we have circumvented the effect of subtle changes in the bonding of the constituent cations. It is surprising that although extensive anion disorder is observed in series such as  $Nd_{2-x}Ho_xZr_2O_7$  it is not observed in the present sample of  $Gd_2Zr_2O_7$ . This highlights the significant difficulty in reconciling the results of various researchers—that is the anion disorder in Zr pyrochlores is sensitive to the precise conditions used to prepare the sample. Fortunately the structure of well ordered  $Gd_2Zr_2O_7$  does not show any significant changes upon cooling to 4 K so that it appears reasonable to use structural information obtained under ambient conditions in the analysis of damage induced by heavy ion bombardment at low temperatures.

In summary we have presented the first accurate and precise structural study of  $Gd_2Zr_2O_7$ . This was achieved using high resolution powder neutron diffraction of a sample enriched in  $^{160}Gd$ . We show it is possible to form well ordered samples of  $Gd_2Zr_2O_7$ . It is expected that disorder [7,13,34] will increase as the structure tends towards the ideal fluorite structure, with  $x_{48f}=0.375$ . As the structure approaches the ideal, ordered pyrochlore structure, radiation-induced amorphization is more easily attained [14]. This raises the question—does introducing anion disorder result in a shift in the position of the 48f anion, and if so does this result in measurable changes in the response of the material to radiation? Future work will endeavour to answer this question.

## Acknowledgments

BJK acknowledges the receipt of a grant from the Australian Institute of Nuclear Science and Engineering that enabled the purchase of the  $^{160}Gd_2O_3$  and from the Australian Research Council.

## References

- [1] A.J. Burggraaf, T. van Dijk, M.J. Verkerk, *Solid State Ionics* 5 (1981) 519.
- [2] M. Lang, F.X. Zhang, J.M. Zhang, J.W. Wang, J. Lian, W.J. Weber, B. Schuster, C. Trautmann, R. Neumann, R.C. Ewing, *Nuclear Instruments & Methods in Physics Research Section B—Beam Interactions with Materials and Atoms* 268 (2010) 2951.
- [3] S. Lutique, D. Staicu, R.J.M. Konings, V.V. Rondinella, J. Somers, T. Wiss, *Journal of Nuclear Materials* 319 (2003) 59.
- [4] J.M. Zhang, M. Lang, J. Lian, J. Liu, C. Trautmann, S. Della-Negra, M. Toulemonde, R.C. Ewing, *Journal of Applied Physics* (2009) 105.
- [5] M.A. Subramanian, G. Aravamudan, G.V.S. Rao, *Progress in Solid State Chemistry* 15 (1983) 55.
- [6] T. Moriga, A. Yoshiasa, F. Kanamaru, K. Koto, M. Yoshimura, S. Somiya, *Solid State Ionics* 31 (1989) 319.
- [7] J. Lian, X.T. Zu, K.V.G. Kutty, J. Chen, L.M. Wang, R.C. Ewing, *Physical Review B* 66 (2002) 054108.
- [8] B.P. Mandal, S.K. Deshpande, A.K. Tyagi, *Journal of Materials Research* 23 (2008) 911.
- [9] Y.H. Lee, J.M. Chen, J.F. Lee, H.C.I. Kao, *Journal of the Chinese Chemical Society* 56 (2009) 543.
- [10] D. Michel, M. Perez, Y. Jorba, R. Collongues, *Materials Research Bulletin* 9 (1974) 1457.
- [11] J.M. Zhang, J. Lian, F.X. Zhang, J.W. Wang, A.F. Fuentes, R.C. Ewing, *Journal of Physical Chemistry C* 114 (2010) 11810.
- [12] L. Minervini, R.W. Grimes, Y. Tabira, R.L. Withers, K.E. Sickafus, *Philosophical Magazine A—Physics of Condensed Matter Structure Defects and Mechanical Properties* 82 (2002) 123.
- [13] K.E. Sickafus, L. Minervini, R.W. Grimes, J.A. Valdez, M. Ishimaru, F. Li, K.J. McClellan, T. Hartmann, *Science* 289 (2000) 748.
- [14] J. Lian, K.B. Helean, B.J. Kennedy, L.M. Wang, A. Navrotsky, R.C. Ewing, *Journal of Physical Chemistry B* 110 (2006) 2343.
- [15] B.P. Mandal, P.S.R. Krishna, A.K. Tyagi, *Journal of Solid State Chemistry* 183 (2010) 41.
- [16] B.P. Mandal, A. Banerji, V. Sathe, S.K. Deb, A.K. Tyagi, *Journal of Solid State Chemistry* 180 (2007) 2643.
- [17] R. Clements, M. Avdeev, J.R. Hester, B.J. Kennedy, C.D. Ling, A.P.J. Stampfl, Unpublished 2010; B.J. Kennedy, M. Avdeev, *Australian Journal of Chemistry* 64 (2011) 119.
- [18] K.D. Liss, B. Hunter, M. Hagen, T. Noakes, S. Kennedy, *Physica B—Condensed Matter* 385–86 (2006) 1010.
- [19] A.C. Larson, R.B. Von Dreele, Los Alamos National Laboratory Report LAUR 86-748, 1994.
- [20] B.H. Toby, *Journal of Applied Crystallography* 34 (2001) 210.
- [21] M. Guillaume, P. Fischer, B. Roessli, P. Allenspach, V. Trounov, *Physica C* 235 (1994) 1637.
- [22] C.S. Knee, B.D. Rainford, M.T. Weller, *Journal of Materials Chemistry* 10 (2000) 2445.
- [23] M. Matsuda, A. Kikkawa, K. Katsumata, S. Ebisu, S. Nagata, *Journal of the Physical Society of Japan* 74 (2005) 1412.
- [24] I. Mirebeau, A. Apetrei, I. Goncharenko, D. Andreica, P. Bonville, J.P. Sanchez, A. Amato, E. Suard, W.A. Crichton, A. Forget, D. Colson, *Physical Review B* (2006) 74.
- [25] J.D.M. Champion, A.S. Wills, T. Fennell, S.T. Bramwell, J.S. Gardner, M.A. Green, *Physical Review B* (2001) 64.
- [26] V.F. Sears, *Neutron News* 3 (1992) 26.
- [27] Y.H. Lee, H.S. Sheu, J.P. Deng, H.C.I. Kao, *Journal of Alloys and Compounds* 487 (2009) 595.
- [28] Y. Tabira, R.L. Withers, T. Yamada, N. Ishizawa, *Zeitschrift Fur Kristallographie* 216 (2001) 92.
- [29] W. Somphon, V. Ting, Y. Liu, R.L. Withers, Q. Zhou, B.J. Kennedy, *Journal of Solid State Chemistry* 179 (2006) 2495.
- [30] B.J. Kennedy, B.A. Hunter, C.J. Howard, *Journal of Solid State Chemistry* 130 (1997) 58.
- [31] R.D. Shannon, *Acta Crystallographica Section A* 32 (1976) 751.
- [32] G.R. Facer, M.M. Elcombe, B.J. Kennedy, *Australian Journal of Chemistry* 1993 (1997) 46.
- [33] R.C. Ewing, W.J. Weber, J. Lian, *Journal of Applied Physics* 95 (2004) 5949.
- [34] J. Lian, J. Chen, L.M. Wang, R.C. Ewing, J.M. Farmer, L.A. Boatner, K.B. Helean, *Physical Review B* 68 (2003) 134107.